SYNTHESIS AND CHARACTERIZATION OF IRON OXIDE NANOLEAF BY THERMAL OXIDATION

Syahriza Ismail^{1,*}, Noor Farah Iddayu Abu Bakar¹, Zaleha Mustafa¹, Noor Irinah Omar² and Siti Aida Ibrahim³

¹Faculty of Manufacturing Engineering, Universiti Teknikal Malaysia Melaka, Hang Tuah Jaya, 76100 Durian Tunggal, Melaka, Malaysia

²Faculty of Mechanical and Manufacturing Engineering Technology, Universiti Teknikal Malaysia Melaka, Hang Tuah Jaya, 76100 Durian Tunggal, Melaka, Malaysia

³Faculty of Engineering Technology, Universiti Tun Hussein Onn Malaysia (Campus Pagoh), 84600 Batu Pahat, Johor

*syahriza@utem.edu.my

Abstract. In this work, a simple method for the efficient and rapid synthesis of onedimensional hematite (\alpha-Fe₂O₃) nanostructures is proposed based on a thermal oxidation approach. This technique is to create iron oxide nanoleaf on the iron (Fe) substrate. The oxidation was done at three different temperatures (200-600 °C) by oxidizing the Fe foils in a chamber furnace. The low temperature thermal oxidation at 400 °C for 2 h resulted in the formation of hematite iron oxide with good nanoleaf coverage on the foil surface. The obtained nanostructures physical and structural characteristics were characterize using XRD, and Raman spectroscopy. While their morphological characteristics were observed using the FESEM. It was discovered that when the oxidation period lengthened, the peak intensities in relation to the hematite increased. The duration of heating has a substantial impact on the development and ultimate morphology of hematite. The creation of this nanostructured formation's growth phenomenon was subsequently explained by a surface diffusion mechanism. According to the X-ray diffraction results, the iron oxide nanoleaf was Fe₃O₄ and α -Fe₂O₃ after the oxidation. The dimension of the nanoleaf was found to be 20-60 nm and lengths up to 1 µm. These dimensions are dependent on the oxidation temperature. The activation energy on the crystallographic plane and grain boundary has an impact on how nanostructures grow during oxidation.

Keywords: Iron oxide, thermal oxidation, hematite, nanoleaf

Article Info

Received 6th March 2023 Accepted 10th April 2023 Published 1st May 2023

Copyright Malaysian Journal of Microscopy (2023). All rights reserved.

ISSN: 1823-7010, eISSN: 2600-7444

Introduction

Iron oxide nanostructures are more affordable, have a higher surface area, and are highly conductive. The indirect band gap of the n-type semiconductor iron oxide ranges from 1.9 to 2.2 eV, depending on the production technique [1]. Most iron oxide, however, is nontoxic, corrosion-resistant, and acceptable for use in a variety of applications. Iron oxides are also found in various significant geological and archaeological samples and in some extraterrestrial materials [2]. Iron oxide often occurs in nature as the polymorphs hematite (Fe₂O₃), magnetite (Fe₃O₄), and maghemite (Fe₂O₃). Hematite is a non-toxic, cheap, and abundant form of earth. Particle size, lattice flaws, contaminants, and ion substitution are a few characteristics that affect the magnetic property of hematite. Hematite can be used as a catalyst, in photoelectrochemical cells, and as a photocatalyst. Recently iron oxide has been known to be a promising adsorbent material for heavy metal removal [3]. A few studies have demonstrated that iron oxide has a high adsorption capacity, which occurs through a chemisorption process involving the hydroxyl group on its surface [4-6]. When in the form of nanostructures such as nanowires or nanoleaf the efficiency of the absorption could be doubled. According to research by Ren et al. [7] the porous fiber-like shape of -Fe₂O₃ demonstrated excellent adsorption of Cr(VI) from water, with rapid adsorption kinetics, high adsorption capacity, and good reusability.

Many scientists have been concentrating on creating chemical and physical processes for creating nanostructured materials. High-grade nanoparticles [8], nano-ovals [9], nanobelts [10] and nanowires [11], or other nanostructures have been produced using a variety of synthetic techniques. The oxidation process is known to be the most straightforward, affordable, and capable of producing high stability phases in a direct manner. Other oxide nanostructures such as whiskers, blades, and belts have been comprehensively studied in the oxidation of other metals, such as Cu [12,13] and Zn [14,15]. Hence the marvels of oxide creation from the oxidation of metals are not limited to Fe. Thermal oxidation offers a simpler approach to forming oxide layers on the metal surface. Oxidation reaction can occur either at high temperature or lower temperature which involves the diffusion of oxidant and chemical reaction. The diffusion and reaction will eventually convert the metal surface into metal oxide. By controlling the oxidation parameters, such as oxidation temperature, time, and environment, distinctive nanostructures can be produced. Besides, it also offers high purity and good oxide quality due to the absence of by-product contamination from the reaction as well as no post-treatment required compared to the sol-gel or hydrothermal process [16]. Thus, thermal oxidation is a fascinating method since it is easy, affordable, and capable of producing high-quality direct iron oxide.

Over many years, there has been significant research on the oxidation characteristics of iron. At oxidation temperatures between 400 and 1000 °C, it has been shown that hematite (α-Fe₂O₃) nanowires are seen to emerge from the oxidized surface of iron [17-19]. According to Vesel & Pichelin [17], the Nanowires with a diameter of about 20 nm and several nm lengths grew on the substrate surface at a narrow temperature of about 900 °C. Budiman et al [3] reported that coral-like and nanowire iron oxide nanostructures were produced at 700 and 800 °C. Meanwhile, Bertrand et al. [20] showed that the effect of water vapor influenced low-temperature iron oxidation (260-500 °C). Thus, it is proven that the nanostructures of iron oxide can be formed but at high temperatures with a controlled environment under vapor influence. It is fascinating to study and investigate the possibility of producing nanostructures at low temperatures without supplying any vapor to the process. This would very much lower the cost and create a robust technique.

The temperature plays a major role in determining the types of nanostructures that can be produced. Hence, the impact of time and temperature on thermal oxidation was examined by using a chamber furnace. The purpose is to study the optimum oxidation parameters for the nanoleaf formation at low temperatures (300–400 $^{\circ}$ C) in a regular environment. Upon oxidation, a formation mechanism for Fe₂O₃ nanoleaf is proposed where it is caused by the stress-driven surface diffusion mechanism.

Materials and Methods

High-purity iron foils were processed utilizing ultrasonography and acetone for a number of minutes. After that, they were thoroughly rinsed with deionized water and then dried in an air stream using air gun. The samples were then thermally oxidized for varying lengths of time at varying temperatures (200 °C, 400 °C, and 600 °C, respectively) in a tube furnace. The temperature was ramped up to the target temperature at a rate of 10 °C/min for oxidation periods of 90 and 120 minutes. Field-emission scanning electron microscope (FE-SEM, S4800, Hitachi) connected with an energy dispersive X-ray (EDX) analyzer was used for the morphology and elemental analysis of the nanostructures. The structural properties of nanostructures were determined by using an X-ray diffractometer (X'pert-MPD PW3040, Phillips) with CuK radiation as well as a Raman spectrometer (Uniram 3500) with a laser wavelength of 532 nm.

Results and Discussion

FESEM images of iron oxide (Fe₂O₃) nanoleaf are shown in Figures 1(a) and (b). These nanoleaf was thermally oxidized at 400 °C for 90 and 120 minutes, respectively. As can be observed in Figure 1, growth of the nanostructure begins at the early stage, but after 90 minutes, the nanoleaf still has not completely covered the surface of the iron substrate, presumably because there was not enough time for it to entirely form throughout the iron substrate. The empty space spotted in Figure 1(a) reveals the Fe foil that acts as the substrate for the nanoleaf growth. After 120 minutes of oxidation exposure, the full extent of nanoleaf growth is visible. The leaf will develop into a thin sword shape with sharp points as the amount of nanoleaf on the substrate grows over time. In addition, variations in the oxidation time led to non-uniform in the length, diameter, and tip size of the nanoleaf. The nanoleaf also developed over the substrate's uneven surface, indicating that there is some room for further growth.

Figure 2(a) to (c) represents the image of FESEM for the top surfaces of nanoleaf on the Fe substrate at different temperature. As seen in the figure, temperature also define the growth of size distribution, diameter and type of nanostructure. At 200 °C there is no indication of nanostructure formed on the substrate, as the temperature is not sufficient for the oxidation to occur and it is below the oxidation temperature of iron (Fe). As a result, the formation of oxide layer was not occurring on the Fe substrate as shown in Figure 2(a). However, at 400 °C (Figure 2(b)), nanoleaf development was noticeable. The nanoleaf was found to be α –Fe₂O₃ with typical diameters of 20-60 nm and lengths up to 1 μ m. A few nanorod structures have grown on the substrate, but other structures, such as small leaves, have not appeared on the substrate because the small nanostructures on the substrate were consolidated due to diffusion process. A sample with an oxidation temperature of 600 °C was physically observed to be disintegrated and the majority of the sample had turned red (Figure

2(c)). Furthermore, uncontrolled airflow during heating has worsened the process and the sample oxidized to 600 °C has formed a thicker oxide layer on the substrate.

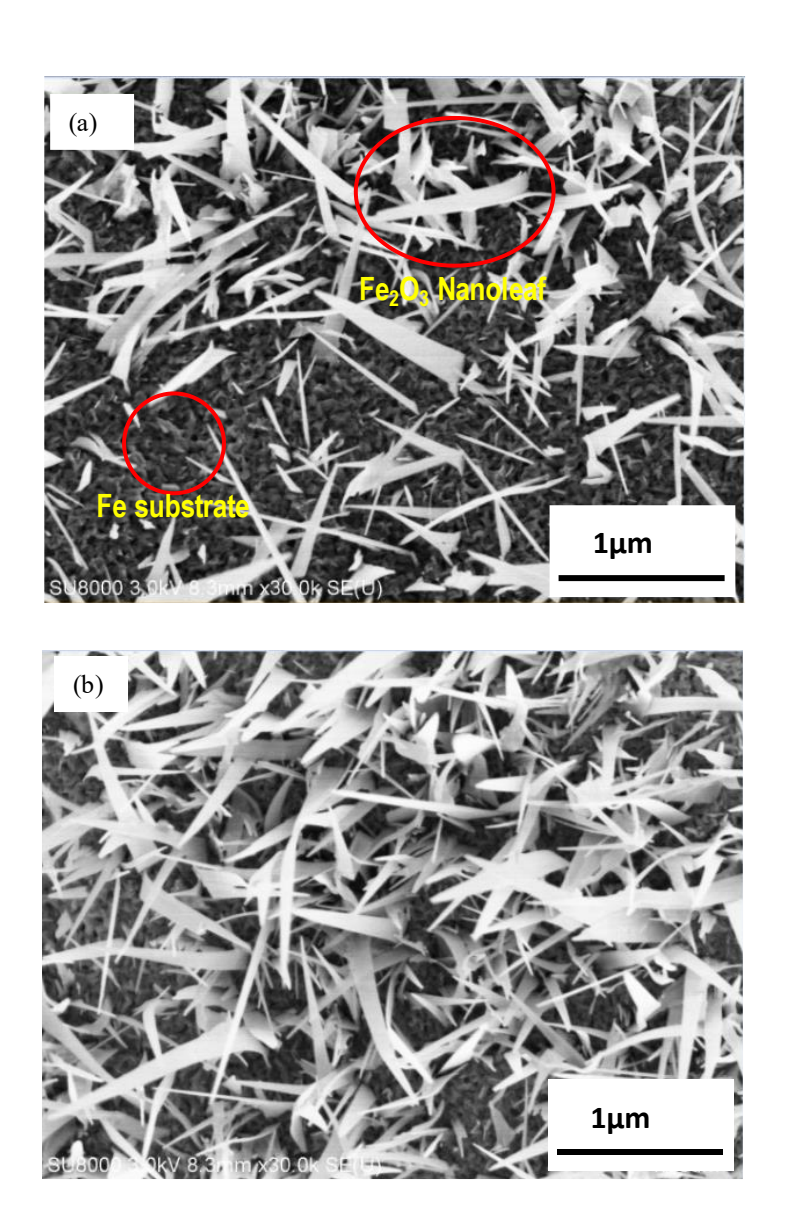


Figure 1: FESEM images of Fe₂O₃ Nanoleaf oxide layer formed by thermal oxidation with time (a) 90 minutes and (b) 120 minutes at 400 °C.

Basically, the driving force that controlled the mobility of the Fe and oxide ion species was what started the formation of the Fe₂O₃ nanoleaf. The existence of potential differences during the oxidation process is due to temperature differences [19]. Fe ions diffuse from the iron substrate core to the surface through the iron oxide interface during the iron oxidation process. Whilst oxide ions diffuse in a reverse way. Figure 3 shows the schematic of nanoleaf formation and the stress-driven mechanism of Fe₂O₃ by diffusion. As seen in the figure, the outward diffusion of Fe ions from the interface of Fe₂O₃ | Fe₃O₄ to the surface is by diffusion reaction at the interface. Then the ions diffuse from the Fe₂O₃ interface to the nanoleaf root and finally to the nanoleaf tip. This process is driven by the ions' concentration gradient.

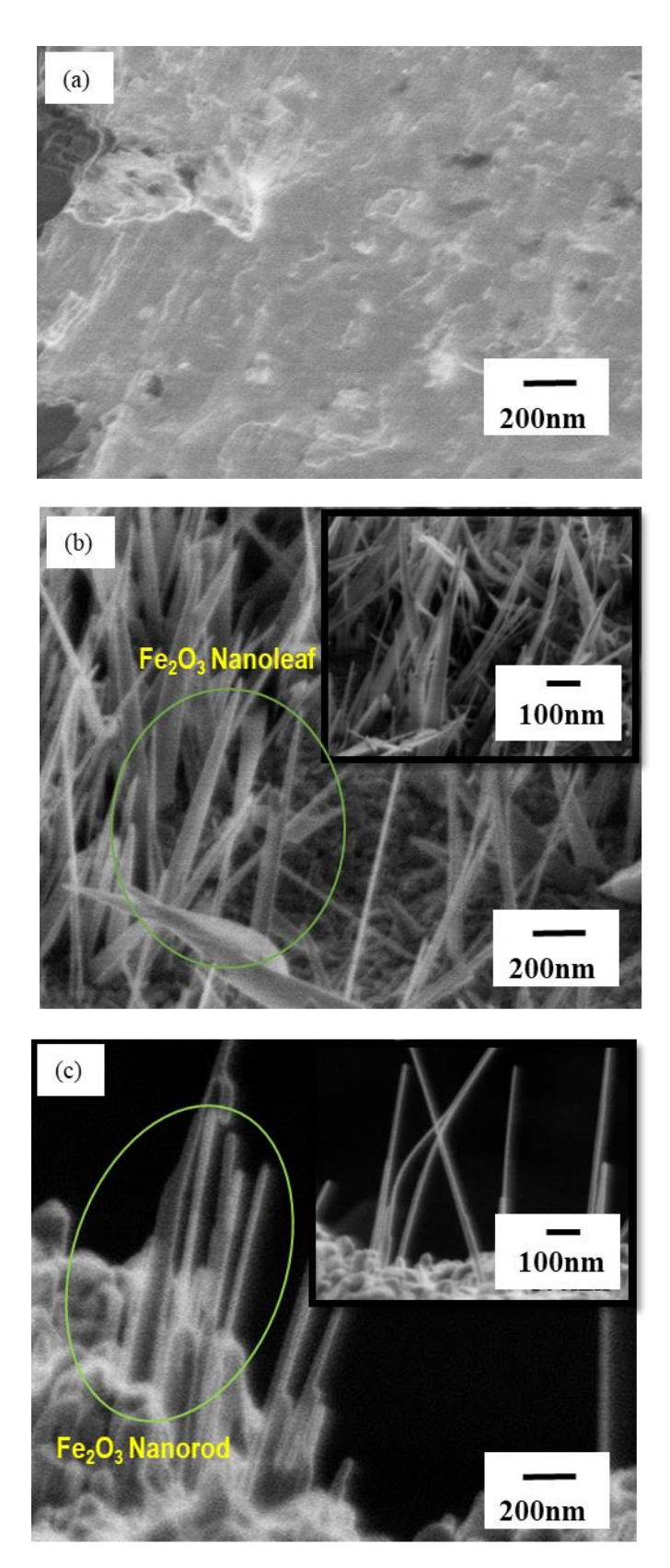


Figure 2: FESEM images of cross sectional Fe₂O₃ nanoleaf at different temperatures (a) 200 °C (b) 400 °C and (c) 600 °C

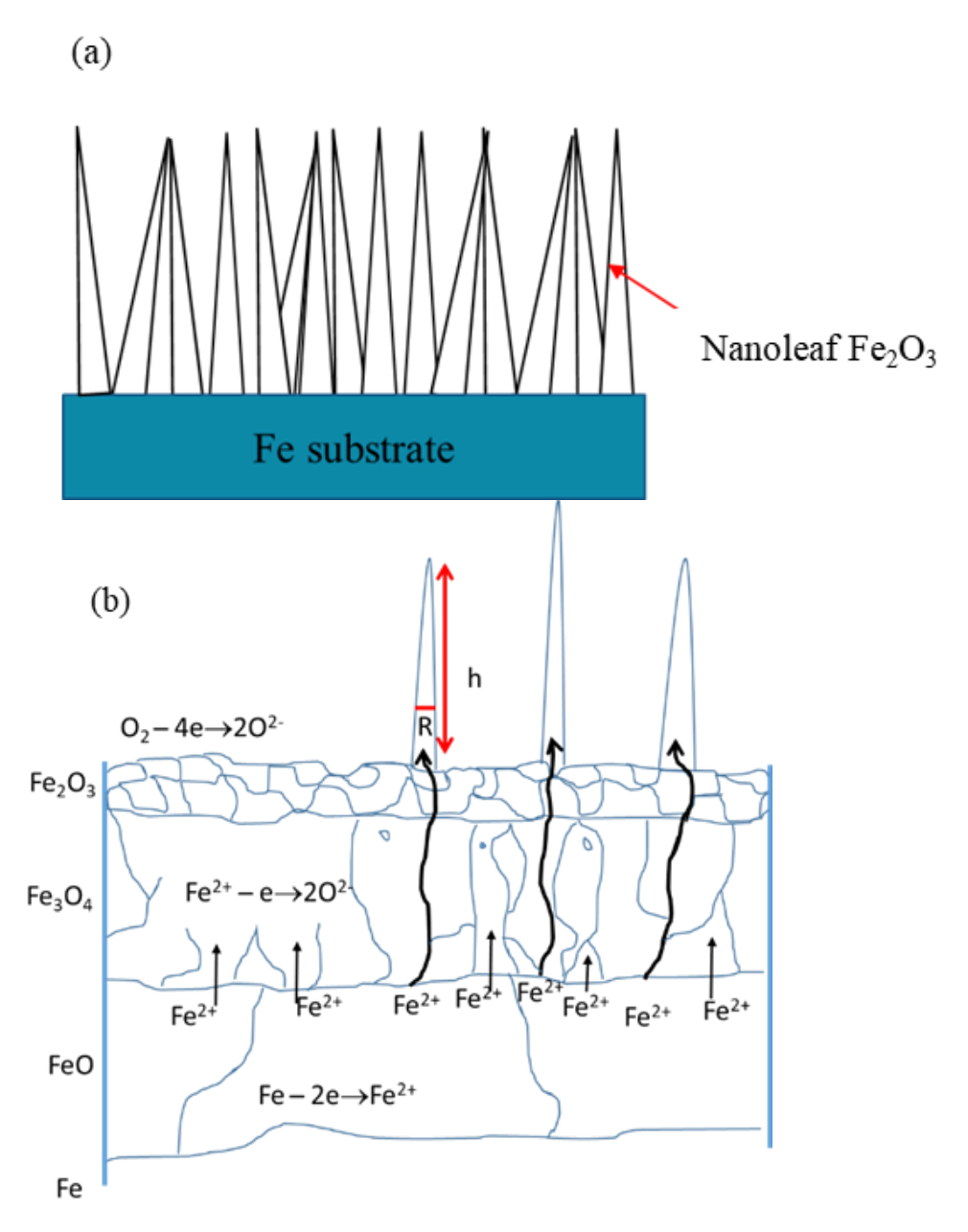


Figure 3: Representation of (a) nanoleaf formation and (b) stress-driven mechanism of Fe₂O₃ nanoleaf growth by diffusion

Furthermore, at specific temperatures, the oxidation stress that causes higher diffusion rates than lattice diffusion is probably the reason for the grain boundaries in the FeO and Fe₃O₄ layers to develop. Besides, in the first part, Fe₂O₃ phase might grow in all directions but further growth only occurs in the [110] crystallographic direction. This is because the direction is the most favorable, as it is much easier for diffusion and stacking. The diffusion rate is enhanced in crystal defects like stacking faults at elevated temperatures [13]. Surface diffusion is another method for getting Fe ions to the top of the Fe₂O₃ nanoleaf. Then, the nanoleaf's sword-like structure, is wider at the bottom and gets thinner at the top. This indicates that the growth is controlled by a diffusion process that originates at the bottom of the leaves. According to the illustration (Figure 3), R represents the nanoleaf's radius and h represents its length.

Figure 4 shows the XRD pattern of 90 and 120 minutes at 400 °C. The patterns show that as time increases, there are more peaks to be found. The peak intensity changed over time as well. Fe peak, though, may also be seen at 65.62° , at 90 and 120 seconds. Hematite Fe₂O₃ peaks present at $2\theta = 35.831^{\circ}$ (110), 43.766° (202), 49.940° (024), and 65.144° (300). However, the peaks of Fe were too intense that has made the Fe₂O₃ become less prominent.

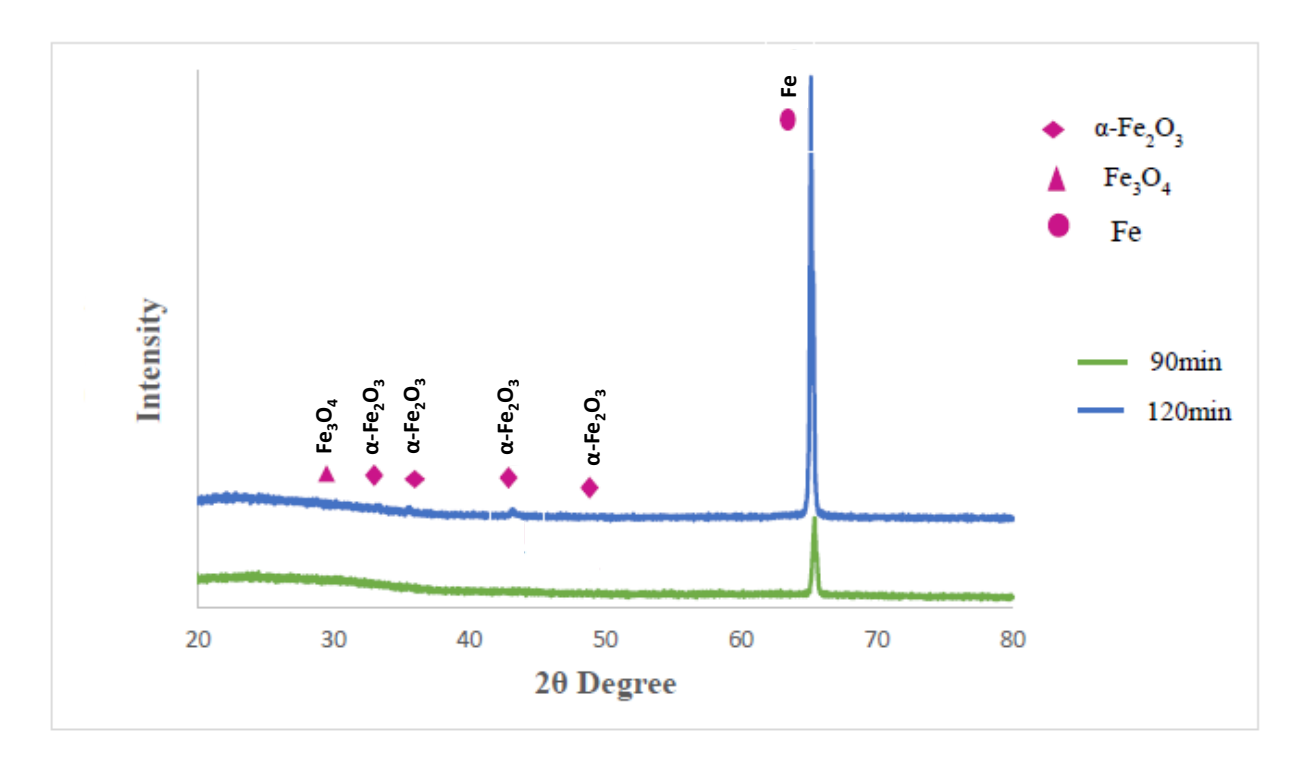


Figure 4: XRD patterns for Fe₂O₃ Nanoleaf oxide layer formed by thermal oxidation at (a) 90 min and 120 min at 400°C

The Raman spectra for 90 and 120 minutes at 400 °C are shown in Figure 4. It should be noted that the ideal conditions for forming a nanostructure on an oxide layer are 400 °C for 90 minutes. The bands at 227, 245, 293, 412, 499, and 612 cm⁻¹, correspond to the α -Fe₂O₃ phase [21]. A similar result is reported by Budiman et al [3] where they concluded that the outermost oxide layer was α -Fe₂O₃ since Raman laser penetration is lower than XRD. As there were no additional peaks, the Raman peaks for 90 and 120 minutes were equal, but the intensity increased at 120 minutes compared to 90 minutes of oxidation. The intensity of the peak relative to the hematite peaks, which is seen to be increased with oxidation time and Hematite is the most stable form of iron oxide. Meanwhile, the lowest oxidizing time induces magnetite or Fe₃O₄.

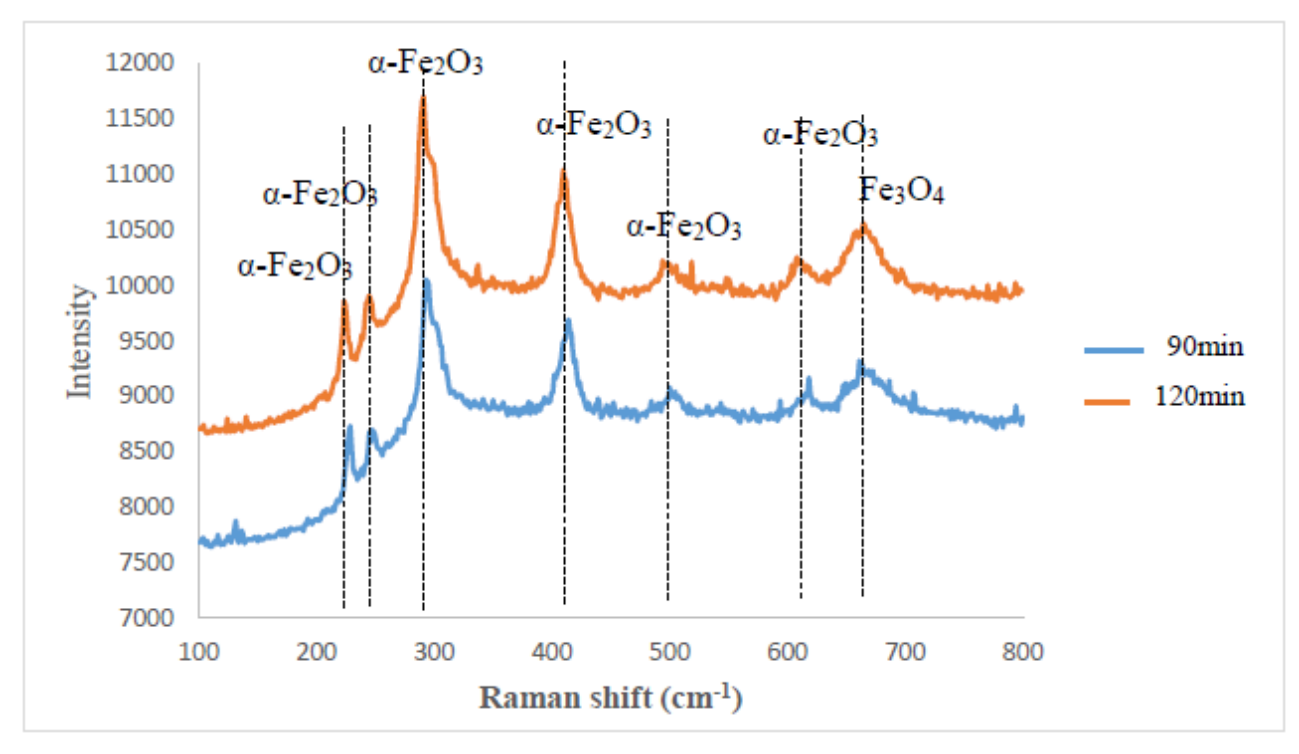


Figure 5: Raman spectrum for iron oxide formed by thermal oxidation process with time at 400 °C in air condition.

Conclusions

In this work, the α - Fe₂O₃ nanoleaf was successfully formed on pure Fe foils by using thermal oxidation at low temperatures. The stable form of iron oxide can be formed when the Fe was oxidized at 400 °C for 2 h. In terms of Fe₂O₃ nanoleaf growth, the mechanism of the reaction process has been observed. The formation mechanism is due to the effect of growth time. As time increase, the nanostructure change from nanoleaf to nanowire and the width of the nanostructure become smaller. The Fe₂O₃ nanoleaf structure can be achieved at 400 °C but as long as the temperature increases, the length of nanoleaf will become longer.

Acknowledgements

The authors gratefully acknowledge Universiti Teknikal Malaysia Melaka (UTeM) for the financial support (S01871) and the Faculty of Manufacturing Engineering, for providing the laboratory facilities.

Author Contributions

All authors contributed toward data analysis, drafting and critically revising the paper and agree to be accountable for all aspects of the work.

Disclosure of Conflict of Interest

The authors declare no potential conflict of interest in the publication of this work.

Compliance with Ethical Standards

The work is compliant with ethical standards

References

- [1] Dlugosch, T., Chnani, A., Muralidhar, P., Schirmer, A., Biskupek, J. & Strehle, S. (2017). Thermal oxidation synthesis of crystalline iron-oxide nanowires on low-cost steel substrates for solar water splitting. *Semiconductor Science and Technology*, 32(8), 084001.
- [2] Vincent, T., Gross, M., Dotan, H. & Rothschild, A. (2012). Thermally oxidized iron oxide nanoarchitectures for hydrogen production by solar-induced water splitting. *International Journal of Hydrogen Energy*, 37(9), 8102-8109.
- [3] Budiman, F., Tan, W. K., Kawamura, G., Muto, H., Matsuda, A., Abdul Razak, K. & Lockman, Z. (2021). Formation of Dense and High-Aspect-Ratio Iron Oxide Nanowires by Water Vapor-Assisted Thermal Oxidation and Their Cr (VI) Adsorption Properties. *ACS Omega*, 15, 6(42), 28203-28214.
- [4] Khan, F.S., Mubarak, NM., Khalid, M., Walvekar, R., Abdullah, E.C., Mazari S.A., Nizamuddin, S. & Karri, R.R.(2020). Magnetic nanoadsorbents' potential route for heavy metals removal—a review. *Environmental Science and Pollution Research*. 27, 24342-24356.
- [5] Singaraj, S.G., Mahanty, B., Balachandran, D. & Padmaprabha, A. (2019). Adsorption and desorption of chromium with humic acid coated iron oxide nanoparticles. *Environmental Science and Pollution Research*. 26, 30044-30054.
- [6] Sruthi, P.D., Sahithya, C.S., Justin, C., SaiPriya, C., Bhavya, K.S., Senthilkumar, P. & Samrot, A.V. (2019). Utilization of chemically synthesized super paramagnetic iron oxide nanoparticles in drug delivery, imaging and heavy metal removal. *Journal of Cluster Science*. 30(1), 11-24.
- [7] Ren, T., He, P., Niu, W., Wu, Y., Ai. L. & Gou, X. (2013). Synthesis of α-Fe₂O₃ nanofibers for applications in removal and recovery of Cr (VI) from wastewater. *Environmental Science and Pollution Research*. 20, 155-162.
- [8] Hassanjani-Roshan, A., Vaezi, M. R., Shokuhfar, A. & Rajabali, Z. (2011). Synthesis of iron oxide nanoparticles via sonochemical method and their characterization. *Particuology*, 9(1), 95-99.
- [9] Wang, X., Wu, X. L., Guo, Y. G., Zhong, Y., Cao, X., Ma, Y. & Yao, J. (2010). Synthesis and lithium storage properties of Co3O4 nanosheet-assembled multishelled hollow spheres. *Advanced Functional Materials*, 20(10), 1680-1686.

- [10] Guan, C., Liu, J., Cheng, C., Li, H., Li, X., Zhou, W., Zhang, H. & Fan, HJ. (2011). Hybrid structure of cobalt monoxide nanowire@ nickel hydroxidenitrate nanoflake aligned on nickel foam for high-rate supercapacitor. *Energy & Environmental Science*. 4(11), 4496-4499.
- [11] Lupan, O., Postica, V., Wolff, N., Polonskyi, O., Duppel, V., Kaidas, V., Lazari, E., Ababii, N., Faupel, F., Kienle, L. & Adelung, R. (2017). Localized synthesis of iron oxide nanowires and fabrication of high performance nanosensors based on a single Fe₂O₃ nanowire. *Small.* 13(16), 1602868.
- [12] Xiang, L., Guo, J., Wu, C., Cai, M., Zhou, X. & Zhang, N. (2018). A brief review on the growth mechanism of CuO nanowires via thermal oxidation. *Journal of Materials Research*. 33(16), 2264-2280.
- [13] Gonçalves, A. M. B., Campos, L. C., Ferlauto, A. S. & Lacerda, R. G. (2009). On the growth and electrical characterization of CuO nanowires by thermal oxidation. *Journal of Applied Physics*, 106(3), 034303.
- [14] Cui, J. (2012). Zinc oxide nanowires. *Materials Characterization*. 64, 43-52.
- [15] Khanlary, M.R., Vahedi, V. & Reyhani, A. (2012). Synthesis and characterization of ZnO nanowires by thermal oxidation of Zn thin films at various temperatures. *Molecules*. 2;17(5), 5021-5029.
- [16] Hasany, S.F., Ahmed, I., Rajan, J. & Rehman A. (2012). Systematic review of the preparation techniques of iron oxide magnetic nanoparticles. *Nanoscience and Nanotechnology* 2(6), 148-158.
- [17] Vesel, A. & Balat-Pichelin, M. (2014). Synthesis of iron-oxide nanowires using industrial-grade iron substrates. *Vacuum*. 100, 71-73.
- [18] Hiralal, P., Unalan. H.E., Wijayantha, K.G., Kursumovic, A., Jefferson, D., MacManus-Driscoll, J.L. & Amaratunga, G.A. (2008). Growth and process conditions of aligned and patternable films of iron (III) oxide nanowires by thermal oxidation of iron. *Nanotechnology*. 19(45), 455608.
- [19] Krajewski, M., Brzozka, K., Lin, W.S., Lin, H.M., Tokarczyk, M., Borysiuk, J., Kowalski, G. & Wasik, D. (2016). High temperature oxidation of iron–iron oxide core–shell nanowires composed of iron nanoparticles. *Physical Chemistry Chemical Physics*. 18(5), 3900-3009.
- [20] Bertrand, N., Desgranges, C., Poquillon, D., Lafont, M.-C. & Monceau, D. (2010). Iron oxidation at low temperature (260–500 C) in air and the effect of water vapor. *Oxidation of Metals*. 73(1-2), 139-162.
- [21] Taniguchi, K. & Kitazawa, N. (2020). Characterization of α-Fe₂O₃ nanorod arrays prepared by a quasi-topotactic transformation of solvothermal derived β-FeOOH nanowire-like arrays. *Journal of Physics and Chemistry of Solids*. 1(147), 109632.